Available online at www.sciencedirect.com
SCIENCE DIRECT
International Journal of Mass Spectrometry 253 (2006) 71–78
International Journal of Mass Spectrometry
www.elsevier.com/locate/ijms

SIMS analysis with neutral cesium deposition: Negative secondary ion sensitivity increase and quantification aspects

P. Philipp [a,*], T. Wirtz [a], H.-N. Migeon [a], H. Scherrer [b]

[a] *Laboratoire d'Analyse des Matériaux, Centre de Recherche Public—Gabriel Lippmann, 41 rue du Brill, L-4422 Belvaux, Luxembourg*
[b] *Laboratoire de Physique des Matériaux, Ecole des Mines, Parc de Saurupt, F-54042 Nancy Cedex, France*

Received 6 January 2006; received in revised form 20 February 2006; accepted 20 February 2006
Available online 23 March 2006

Abstract

To overcome the SIMS matrix effect in the negative secondary ion mode, analyses can be performed on the Cation Mass Spectrometer using neutral cesium deposition with simultaneous primary ion bombardment. This paper discusses the advantages of this technique by applying it on several samples. The useful yields of various elements detected as negative secondary ions are calculated and discussed in terms of work function and electron affinity. The additional Cs deposition allows a significant increase of the useful yields of negative secondary ions and thus of the analysis sensitivity compared to traditional Cs^+ primary ion bombardment. At maximal cesium surface concentrations, quantitative analyses become possible for elements with high electron affinities. For other elements a significant increase of the analysis sensitivity is achieved.
© 2006 Elsevier B.V. All rights reserved.

Keywords: SIMS; Neutral cesium deposition; Useful yield; Quantification; Cation Mass Spectrometer

1. Introduction

Owing in particular to its excellent sensitivity, its high dynamic range and its good depth resolution, Secondary Ion Mass Spectrometry (SIMS) constitutes an extremely powerful technique for analyzing surfaces and thin films. Today, SIMS is widely used for analysis of trace elements in solid materials, especially semiconductors and thin films. Other emerging fields of application for SIMS are biology and medicine in particular.

At the same time the SIMS technique is hampered by a major deficiency which is the lack of quantification due to the matrix effect [1]: the ionization probability of secondary ions and thus the sensitivity of the analysis depends on the sample composition. In fact, the emission of secondary ions is very sensitive to the chemical state of the sample surface [1–3]. After reacting with electropositive elements, most surfaces exhibit drastically enhanced negative secondary ion yields [4]. These yields might be higher by several orders of magnitude than the yields from the respective clean surfaces.

It has been shown that the deposition or incorporation of alkali metals on surfaces of metals or semiconductors leads to a decrease of the electron work function of the sample [5–9] and induces an increase of the negative secondary ion sensitivity [10,11].

Because of the aforementioned reasons, Cs^+ bombardment is widely employed in SIMS analyses to effect this negative ion yield enhancement, thus providing higher detection sensitivities. Previous studies have shown that the negative ion yields strongly depend on the stationary cesium surface concentration incorporated in the specimen during the primary bombardment [4,10,12–14]. On commercial dynamic SIMS instruments the primary Cs^+ bombardment serves both for the incorporation of Cs in the material and for the sputtering of the surface. In this case, the primary bombardment conditions (mainly the impact energy and the incidence angle, which can be adapted only in a very limited way on conventional SIMS equipment) as well as the characteristics of the investigated specimen imply a distinct total sputtering yield Y and consequently determine the cesium surface concentration. As a consequence, the Cs concentration is practically fixed for a given type of sample and cannot be chosen freely. Studies examining the effect of Cs concentration on negative ion sensitivities were hence mainly limited to the Cs surface concentration evolution in the transient regime or to

* Corresponding author. Tel.: +352 47 02 61 559; fax: +352 47 02 64.
E-mail address: philipp@lippmann.lu (P. Philipp).

1387-3806/$ – see front matter © 2006 Elsevier B.V. All rights reserved.
doi:10.1016/j.ijms.2006.02.018

Cs surface concentrations obtained by different bombardment conditions [10,14].

The Cation Mass Spectrometer (CMS), which is a SIMS prototype developed in our laboratory, has been designed to overcome this problem [15–20]. This instrument is equipped with a patented neutral cesium Cs^0 evaporator [21] to vary the Cs surface concentration over the whole range and to ensure an optimal Cs surface concentration for maximum negative secondary ion sensitivity. In that way Cs surface concentration adjustment is decoupled from primary ion bombardment and the primary ion type can be chosen with respect to the application.

In the past, neutral Cs^0 deposition and simultaneous ion irradiation has already been used to study the effect of Cs enrichment on secondary ion ionization processes, but sensitivities could not be determined [22–24].

In this paper, Cs^0 deposition with simultaneous ion bombardment is used to study sensitivity evolutions of negative secondary ions with respect to the Cs surface concentrations. For a better understanding, the experimental results will be compared to existing models and the usefulness and the limits of the technique will be shown by several applications.

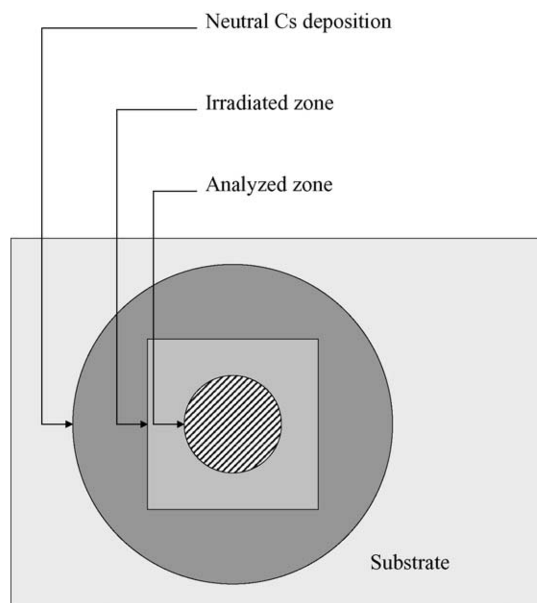

Fig. 1. Diagram defining Cs deposition zone, irradiated zone and analyzed zone.

2. Experimental

The design and the main characteristics of the CMS have already been published in previous works [15,16].

At the moment the CMS is equipped with two ion guns and a patented neutral Cs^0 evaporator which has been developed in LAM. The LMIS Ga^+ was operated with an impact energy of 32.5 keV and currents between 100 pA and 5 nA. In order to be able to vary the erosion rate, we changed the density of bombardment with Ga^+ ions by adapting the dimensions of the scanning surface. The primary beam was thus raster-scanned across a quadratic area varying from 25 μm × 25 μm to 100 μm × 100 μm. The Cs^+ sputter ion gun was run with an impact energy of 13 keV and currents ranging between 3 nA and 19 nA. Again, the dimensions of the rastered area were varied between 30 μm × 30 μm and 300 μm × 1200 μm. The neutral Cs deposition rates of the evaporator, which were measured by means of a quartz microbalance system, changed between 0.4 Å/s and 3.0 Å/s. During the experiments, Cs^0 deposition was used simultaneously with one of the aforementioned ion guns.

The sample was positioned at a distance $d = 3.5$ mm from the extraction nose and polarized to −4500 V.

For these series of measurements, secondary ions were accepted from a circular area on the sample surface limited to a diameter of 22 μm or 42 μm, defined by an aperture centered with respect to the scanning area. Cs^0 is deposited on a still larger area that is centered on the area irradiated by the ion beam (Fig. 1). The mass spectrometer was operated at a mass resolution of $M/\Delta M = 300$ and with an energy bandpass $\Delta E = 130$ eV.

To study the useful yield variations with respect to the Cs concentration C_{Cs} and to observe the influence of the sample work function Φ on ionization, we opted for samples of aluminum, silicon and nickel, given that these materials cover a considerable range on the work function scale: $\Phi_{Al} = 4.28$ eV [25], $\Phi_{Si} = 4.85$ eV [25] and $\Phi_{Ni} = 5.15$ eV [26]. These samples were compared to binary compounds (GaAs and InP). Only the work function of GaAs could be found in literature ($\Phi_{GaAs} = 5.3$ eV) [8]. Si, GaAs and InP were mono-crystalline samples whereas Al and Ni were polycrystalline.

For a large number of different erosion rates and Cs^0 deposition rates, we performed depth profiles on the five studied samples while detecting the M^- signals emitted from the respective surfaces.

At the end of the analyses, the post-bombardment craters were measured with a Tencor P-10 profilometer.

3. Results

3.1. Definitions

The secondary ion sensitivities are discussed in terms of useful yield, which is defined by:

$$\mathrm{UY}(\mathrm{M}^-) = \frac{\text{number of detected M}^- \text{ ions}}{\text{number of sputtered M atoms}} \quad (1)$$

For matrix elements, this relation becomes in the equilibrium state:

$$\mathrm{UY}(\mathrm{M}^-) = \frac{I_s t}{(\pi/4) d\rho\varphi^2 R} \quad (2)$$

where I_s denotes the secondary ion current intensity, t the acquisition time, d the crater depth, ρ the atomic density of the sample, φ the diameter of the analyzed zone and R is the isotopic ratio.

As the Cs surface concentration cannot be determined in situ, it will be described by characteristic parameters and it is considered to be a mean surface concentration in a volume close to the sample surface. For Ga^+ bombardment and Cs^0 deposition (Ga^+/Cs^0 bombardment), the Cs surface concentration C_{Cs} is

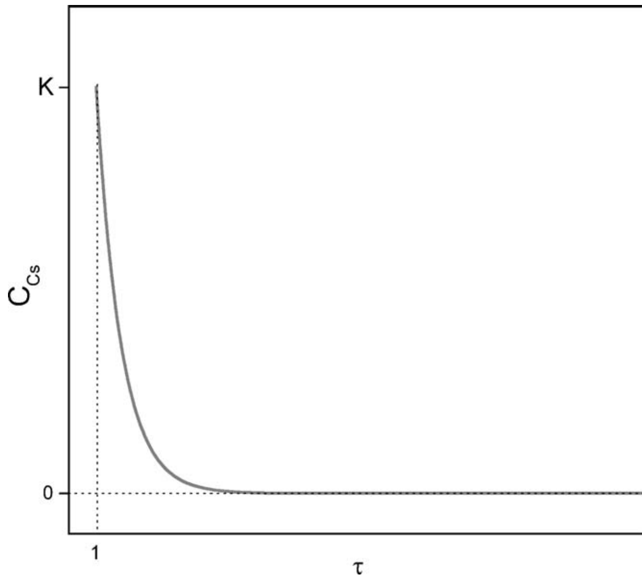

Fig. 2. Calculated Cs surface concentration evolution with respect to parameter τ for Ga^+/Cs^0 bombardment.

defined by:

$$C_{Cs} = \frac{n_{Cs}}{n_{Cs} + n_M + n_{Ga}} \quad (3)$$

where n_{Cs} is the number of Cs atoms deposited on the irradiated area, n_M the number of atoms M that are sputtered from the sample and n_{Ga} is the number of Ga^+ ions that have been implanted by the primary Ga^+ bombardment. Cesium can mainly be found at the surface of the sample and to a lesser degree in the sample as a consequence of atomic mixing.

For Ga^+/Cs^0 bombardment, the Cs surface concentration is defined by the parameter τ which depends only on analytical parameters that can be determined easily [27]:

$$\tau = \frac{v_{erosion}}{v_{deposition}} \quad (4)$$

where $v_{erosion}$ is the erosion velocity and $v_{deposition}$ is the Cs^0 deposition velocity. The erosion rate is calculated by considering the sputtering time and the depth of the crater.

The typical C_{Cs} behavior with respect to parameter τ is shown in Fig. 2. C_{Cs} is a function of the parameter τ and not of $v_{deposition}$ and $v_{erosion}$ taken individually [27]. K in Fig. 2 indicates the maximum Cs surface concentration that can be reached by Ga^+/Cs^0 bombardment.

For Cs^+ bombardment and Cs^0 deposition (Cs^+/Cs^0 bombardment) the situation is similar. The Cs surface concentration is defined by:

$$C_{Cs} = \frac{n_{Cs^0}}{n_{Cs^0} + n_M + n_{Cs^+}} + \frac{1}{1+Y} \quad (5)$$

where n_{Cs^+} is the number of Cs^+ ions that has been implanted by the primary bombardment and Y is the sputtering yield. The first part of the equation represents the contribution to C_{Cs} due to Cs^0 deposition, while the second part is due to the contribution of Cs^+ bombardment. Analogously to relation (4), we define the

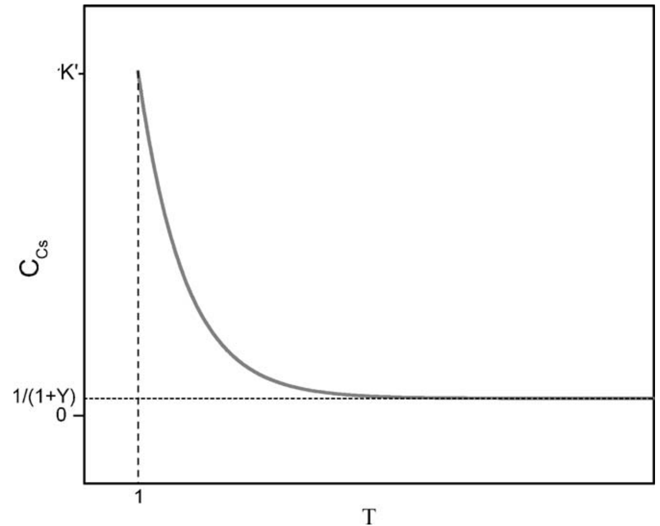

Fig. 3. Calculated Cs surface concentration evolution with respect to parameter T for Cs^+/Cs^0 bombardment.

characteristic parameter T:

$$T = \frac{v_{erosion}}{v_{deposition}} \quad (6)$$

The evolution of C_{Cs} with respect to parameter T is plotted in Fig. 3. Again C_{Cs} is a function of parameter T and not of $v_{deposition}$ and $v_{erosion}$ taken individually. K' in Fig. 3 indicates the maximum Cs surface concentration that can be reached by Cs^+/Cs^0 bombardment.

3.2. Ga^+/Cs^0 bombardment

Fig. 4 shows the evolution of Si^- useful yield plotted with respect to $v_{erosion}$. As expected, the useful yield increases for decreasing $v_{erosion}$, that is to say for rising C_{Cs}. This rising of C_{Cs} induces shifts of the electron work function of the Si sample which alter the secondary ion ionization probability according

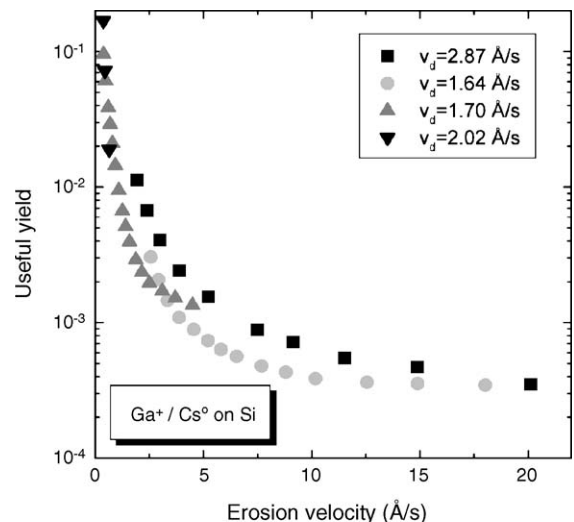

Fig. 4. Si^- useful yield variation with respect to the erosion velocity for Ga^+/Cs^0 bombardment.

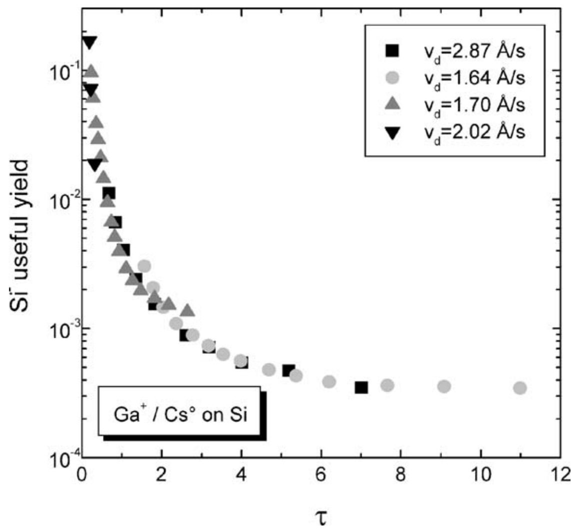

Fig. 5. Si^- useful yield variation with respect to parameter τ for Ga^+/Cs^0 bombardment.

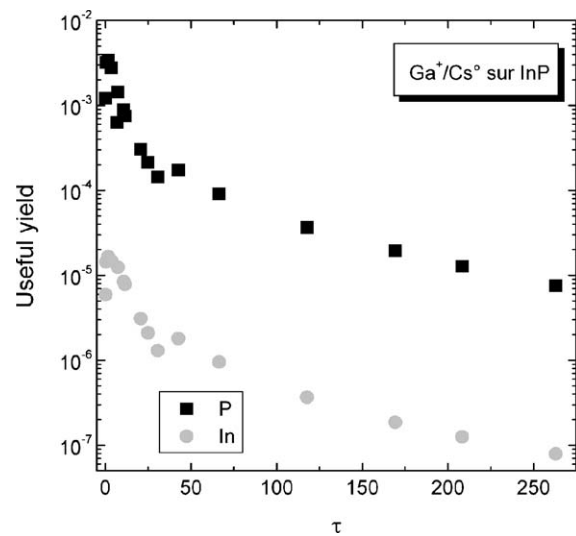

Fig. 6. P^- and In^- useful yield variations with respect to parameter τ for Ga^+/Cs^0 bombardment.

to the electron tunneling model:

$$\begin{cases} \beta_{Si}^- = 1 \text{ if } \phi < A \\ \beta_{Si}^- \propto e^{-(\phi-A)/\varepsilon_n} \text{ if } \phi > A \end{cases} \quad (7)$$

where β_{Si}^- is the secondary ion ionization probability, Φ the work function of the sample, A the electron affinity of the sputtered atom and ε_n is a parameter which is proportional to the normal component of the velocity with which the atoms leave the surface.

One should also note that the different curves of Fig. 4 do not superpose: the useful yield is not a function of $v_{erosion}$ and $v_{deposition}$ taken individually. If the same data are plotted with respect to the parameter τ the different curves lie on each other (Fig. 5) proving that the parameter τ characterizes C_{Cs}.

The Si^- useful yields have been largely increased by Cs^0 deposition. Compared to normal Cs^+ bombardment on the CMS, they increased from 4.3×10^{-3} to 1.6×10^{-1}. One should however note that the flat part of the useful yield curve predicted by Eq. (7) has not been obtained. The most probable explanation for this is that the maximal C_{Cs} reached during our experiments is not high enough to provoke a sufficient decrease of the work function. Higher C_{Cs} can possibly be obtained by Cs^+/Cs^0 bombardment. Nevertheless a maximal useful yield of 0.16 indicates that the ionization must be close to one, as the transmission of the mass spectrometer is about 20% [15].

Ga^+/Cs^0 bombardment on InP and Al samples leads to similar results than Ga^+/Cs^0 bombardment on Si. Figs. 6 and 7 show the useful yield curves with respect to the parameter τ for these samples. For all analyzed elements, the useful yields first increase slowly when τ is decreased. At small values of τ a steep increase of the useful yields can be observed. As for Si, constant values of the useful yield at low values of τ, which would indicate total ionization, cannot be observed. This is however not surprising because the analyzed elements all have lower electron affinities than Si and their negative ionization is thus less probable.

The useful yields obtained during these experiments using neutral Cs deposition are enhanced by about two orders of magnitude compared to "ordinary" SIMS measurements.

The difference between the maximal useful yields of P^- and In^- is due to the different electron affinities of these two elements. P has the highest electron affinity (0.75 eV for P and 0.40 eV for In) and therefore presents the highest useful yield. This behavior is in agreement with the predictions of the electron tunneling model (Eq. (7)).

For Al (Fig. 7), the polycrystalline surface roughened slightly under the primary ion bombardment giving rise to less reproducible useful yields.

For the GaAs and Ni samples finally, primary ion bombardment induced roughness on the bottom of the crater was too important to evaluate the crater volume and made subsequent useful yield calculations impossible. Surface roughness is often induced on surfaces irradiated by ions. The amplitude of the

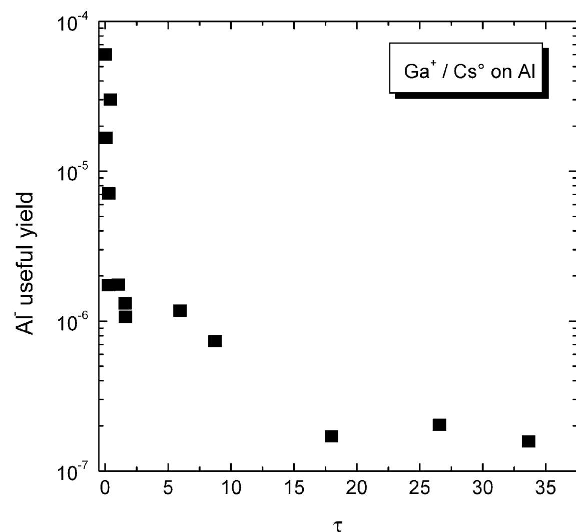

Fig. 7. Al^- useful yield variation with respect to parameter τ for Ga^+/Cs^0 bombardment.

roughness depends on irradiation conditions, ion type and sample composition [28–32]. In our experiments, neutral cesium deposition is observed to increase the surface roughness significantly on the GaAs and Ni samples.

3.3. Cs^+/Cs^0 bombardment

Experiments for Cs^+/Cs^0 bombardment have been carried out in the same way than for Ga^+/Cs^0 bombardment: C_{Cs} is varied over a large range by changing the primary ion current density. This time, Cs is introduced into the sample both by the deposition of Cs^0 on the sample surface and by the Cs^+ ion bombardment. The specific parameter characterizing C_{Cs} is now called T to avoid any confusion with the Ga^+/Cs^0 bombardment mode. For a given value of τ or T, the Cs^+/Cs^0 mode produces logically higher C_{Cs} than the Ga^+/Cs^0 mode due to the extra implantation of Cs by the ion bombardment. As a consequence, for a given value of τ or T, the useful yields of negative secondary ions are higher in the Cs^+/Cs^0 mode than in the Ga^+/Cs^0 mode.

The overall behavior of useful yield variations with respect to the parameter T by Cs^+/Cs^0 bombardment is analogous to the one found for Ga^+/Cs^0 bombardment.

Cs^+/Cs^0 bombardment on Si generates similar useful yields than Ga^+/Cs^0 bombardment on Si (Fig. 8). The useful yield increases first slowly when T is decreased before rising steeply at small values of T. The scattering of useful yield data points at higher values of T are due to reproducibility problems between different series.

Cs^+/Cs^0 bombardment on GaAs and InP produce comparable results (Figs. 9 and 10). The differences between useful yield evolutions for As^- and Ga^- and for P^- and In^- are due to electron affinity differences between the analyzed elements. For each sample, the element with the highest electron affinity shows the greatest useful yield (electron affinities: 0.81 eV for As and 0.75 eV for P compared to 0.43 eV for Ga and 0.40 eV for In).

Useful yield evolutions from the polycrystalline samples Al and Ni are comparable to the other matrixes (Figs. 11 and 12).

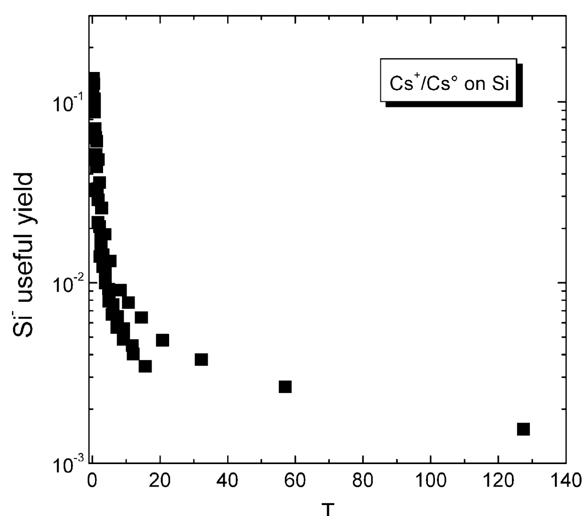

Fig. 8. Si^- useful yield variation with respect to parameter T for Cs^+/Cs^0 bombardment.

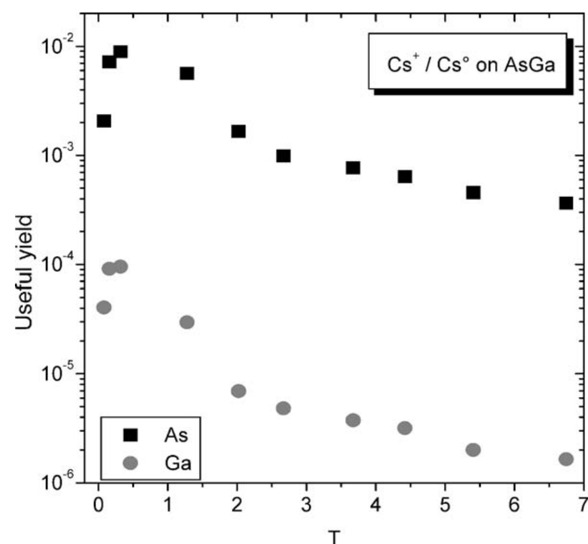

Fig. 9. Ga^- and As^- useful yield variations with respect to parameter T for Cs^+/Cs^0 bombardment.

The reproducibility of the values is however less good due to the formation of roughness on the crater bottoms induced by ion bombardment.

A useful yield gain of several orders is achieved for all samples. Compared to normal Cs^+ bombardment on the CMS, Ga^- useful yield increased from 1.0×10^{-6} to 9.5×10^{-5}, As^- useful yield from 2.8×10^{-4} to 9.0×10^{-3} and Si^- useful yield from 4.3×10^{-3} to 1.3×10^{-1}.

3.4. Generalization and applications

The preceding results of Sections 3.1 and 3.2 show that Cs^0 deposition with simultaneous ion bombardment leads to an important useful yield gain improving the analysis sensitivity by several orders of magnitude. However, the experiments were carried out on samples with a very simple

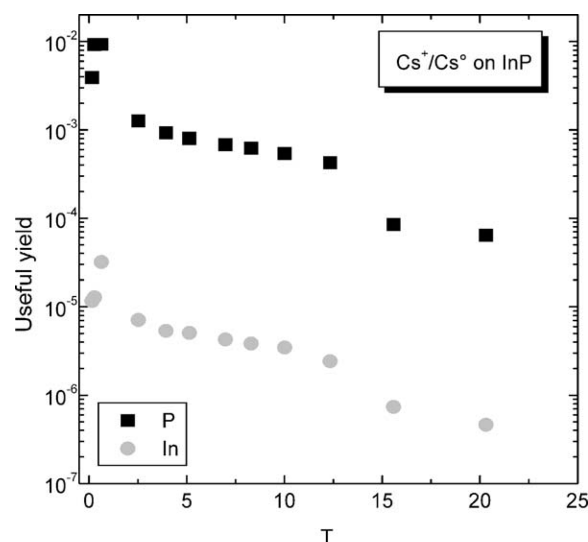

Fig. 10. In^- and P^- useful yield variations with respect to parameter T for Cs^+/Cs^0 bombardment.

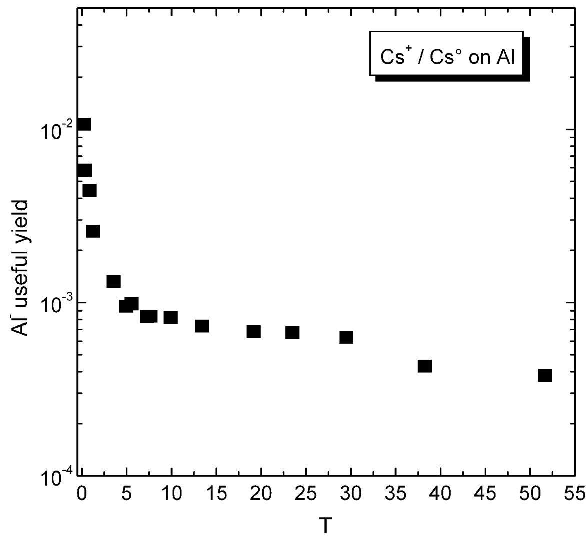

Fig. 11. Al^- useful yield variation with respect to parameter T for Cs^+/Cs^0 bombardment.

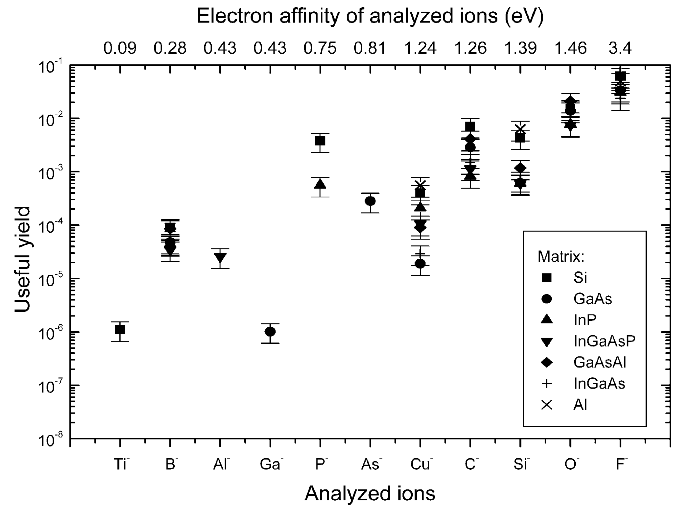

Fig. 13. Useful yields for ions extracted from several matrixes for Cs^+ bombardment.

composition, containing mainly only one element, which makes conclusions regarding the usefulness of this technique for routine applications in SIMS analysis rather complicated. To investigate this problem, ion bombardment with simultaneous Cs^0 deposition was tested on an application: depth profiling and quantification on samples containing known concentrations of implanted elements were realized by Cs^+/Cs^0 bombardment.

The depth profiles were carried out on several matrixes with different work functions in which a large number of elements with varying electron affinities had been previously implanted. By this means, the influence of these parameters on ionization and quantification could be studied. To begin with, the analyses were carried out with Cs^+ bombardment without simultaneous Cs^0 deposition to get the useful yields for the experimental conditions which were standard on the CMS up to now. Only afterwards Cs^+/Cs^0 bombardment was used to observe the useful yield gain enhancements and possibilities for quantification brought about by this technique.

For Cs^+ bombardment, the useful yield dependence on electron affinity of the analyzed element and on sample work function is clearly visible (Fig. 13). On one hand, the useful yields increase with the electron affinity of the analyzed element. On the other hand, for each element, the useful yield is highest for the matrix with the lowest work function (Al and Si). Finally, as can be concluded from the observed variations of the useful yield with respect to the matrix, the matrix effect persists even for the elements with the greatest electron affinity (3.4 eV for F).

For Cs^+/Cs^0 bombardment the situation changes (Fig. 14). Useful yields of the elements with the highest electron affinity become independent of the sample making quantitative analysis possible. The small fluctuations in useful yields can be linked to problems adjusting C_{Cs}. Indeed, at low values of parameter T, useful yields change very rapidly with T so that a small variation of T produces an important change in the useful yield

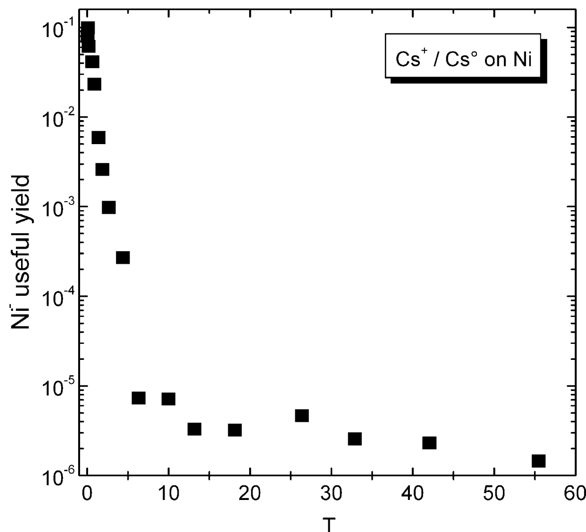

Fig. 12. Ni^- useful yield variation with respect to parameter T for Cs^+/Cs^0 bombardment.

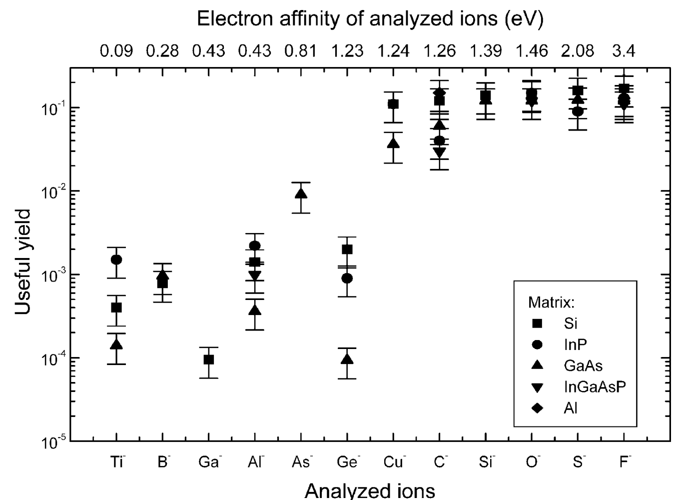

Fig. 14. Useful yields for secondary ions extracted from several matrixes for Cs^+/Cs^0 bombardment.

(Figs. 5–12). At slightly smaller electron affinities (for Cu^- and C^- in Fig. 14) the useful yield is still maximized for samples with low work function but begins to depend on the work function for the other matrixes. For elements with even lower electron affinities a maximization of the useful yield becomes impossible. In spite of these remaining quantification problems for the elements having a low electron affinity, analyses with Cs^+/Cs^0 bombardment lead to significantly better sensitivities compared to the ones obtained with pure Cs^+ bombardment (Fig. 13). So the experimental data in Fig. 14 can be divided in three categories. In the first category ($A > 1.26$), Φ is always smaller than A and ionization is always complete (Eq. (7)). In the second category ($1.23 < A \leq 1.26$), Φ becomes larger than A for some matrixes (for example, GaAs, Fig. 14) bringing about partial ionization for these samples. In the third category ($A \leq 1.23$), Φ is always larger than A and the matrix effect is visible for all samples.

4. Discussion

Maximal useful yields for Ga^+/Cs^0 bombardment and for Cs^+/Cs^0 bombardment obtained for Al, GaAs, InP, Ni and Si as well as the electron affinities A and sample work functions Φ are summarized in Table 1. Compared to traditional Cs^+ bombardment, both, Ga^+/Cs^0 and Cs^+/Cs^0 bombardments cause an important increase of the useful yield resulting in a significant gain of analysis sensitivity. The curves plotting the useful yields of the different elements versus the characteristic parameters τ and T exhibit an exponential growth which corresponds qualitatively to the electron tunneling model predictions and to an experimental behavior found by other author [10,12,22–24,33–36]. The useful yields first increase slowly when the parameters τ and T are lowered (low C_{Cs} region) before rising steeply at low values of τ and T (high C_{Cs} region). A flat part of the curve corresponding to a secondary ion ionization probability equal to 1 cannot be observed.

The different useful yields can be compared most easily by considering the difference $\Phi - A$ which can be found in the electron tunneling model (Eq. (7)). When Cs^0 is deposited on the sample surface, the work function Φ of the sample and consequently the difference $\Phi - A$ decrease. According to the electron tunneling model, low values of $\Phi - A$ should correspond to high useful yields. The useful yields found during our experiments mainly respect this rule (Table 1). For Ga^+/Cs^0 bombardment, Si has the highest useful yield and $\Phi - A$ is lowest for this sample. Work function data or experimental data are missing for InP, Ni and GaAs. The Al^- useful yield is less increased by Cs^0 deposition than the Si^- useful yield. Surface roughness, which made the determination of small crater volumes impossible, prevents higher useful yields from being measured. For Cs^+/Cs^0 bombardment, the useful yield evolution compared to the $\Phi - A$ variation is respected for Si, Ni, As, Al and Ga. Finally, as the useful yields of P^- and In^- are close to the As^- and Ga^- useful yields, the work functions of both samples are probably similar.

Table 1
Useful yield comparison for Ga^+/Cs^0 and Cs^+/Cs^0 bombardment

Element	A (eV)	Φ (eV)	Φ − A (eV)	Ga^+/Cs^0 UY	Cs^+/Cs^0 UY
Si	1.39	4.85	3.46	1.6×10^{-1}	1.3×10^{-1}
Ni	1.16	5.15	3.99	Roughness	9.9×10^{-2}
As (GaAs)	0.81	5.30	4.49	Roughness	9.0×10^{-3}
P (InP)	0.75	–	–	3.0×10^{-3}	8.0×10^{-3}
Al	0.43	4.28	3.85	6.0×10^{-5}	1.1×10^{-2}
Ga (GaAs)	0.43	5.30	4.87	Roughness	9.5×10^{-5}
In (InP)	0.40	–	–	1.6×10^{-5}	8.0×10^{-5}

The table shows the maximum useful yields (corresponding to the lowest values of τ, respectively, T) obtained for the different experimental conditions.

The differences between useful yields for Ga^+/Cs^0 bombardment and Cs^+/Cs^0 bombardment are in general weak (Table 1), indicating that similar maximum Cs surface concentrations are reached for the two bombardment types. The useful yield gains qualitatively correspond to the predictions of the electron tunneling model for $\Phi > A$ (Eq. (7)). As well as for Ga^+/Cs^0 bombardment as for Cs^+/Cs^0 bombardment, Cs surface concentrations are not important enough to lower Φ below A and produce the plateau predicted by the electron tunneling model. For both types of bombardment conditions the influence of the electron affinity of the analyzed element and sample work function on ionization processes are the same. The main difference between the two bombardment conditions is observed at high values of the parameters τ and T where Cs^+/Cs^0 bombardment produces much larger C_{Cs} due to implantation of primary Cs^+ ions (Figs. 5–12). Thus, the useful yield gain due to Cs^0 deposition is most important for Ga^+ bombardment and in general for primary ions different from Cs^+.

A difference between maximal useful yields for the two bombardment conditions can only be observed for Al and InP where Cs^+/Cs^0 bombardment produces a much larger useful yield than Ga^+/Cs^0 bombardment. This is probably due to a more important surface roughness formation at the bottom of the craters for Ga^+/Cs^0 bombardment, which makes the determination of small crater volumes impossible and prevents higher useful yields from being measured.

Figs. 13 and 14 show that quantitative analyses can be performed easily for elements with high electron affinity. For these elements, the matrix effect is eliminated, as the ionization probability does not depend on the matrix composition. On the other hand, the analysis sensitivity for elements with lower electron affinity can be improved significantly but quantification still remains complicated. Consequently quantification is possible for elements with an electron affinity that is at least equal to 1.39 eV. At an electron affinity of 1.26 eV matrix effects remain visible. In between those two values the maximal useful yields and their variations with respect to sample work function stay unidentified.

These experiments show also that the spectrometer transmission for negative secondary ion analyses on the CMS is limited to ≈20%. For elements with maximized ionization probabilities, small useful yield variations between the different elements are due to the spectrometer transmission that depends on the energy distribution of the analyzed element.

Depth profiling produces similar high useful yields than the experiments on matrixes of simple composition and shows that Cs^0 deposition with simultaneous ion bombardment can be

applied to typical SIMS applications. Likewise, ion imaging with Ga^+/Cs^0 bombardment will produce comparable results than depth profiling with Cs^+/Cs^0 bombardment, e.g., quantitative analyses for elements with high electron affinity and better analysis sensitivity for elements with lower electron affinity.

Besides, not all theoretical or fundamental aspects could be discussed in this paper. They are linked to implantation of deposited Cs into the sample by primary ion bombardment, differences in Cs surface concentration or sputtering due to changing primary ions and physical parameters like changing work function with respect to the parameters τ and T. An evaluation of these different points in order to obtain a more complete comparison with theoretical models will be discussed in following papers.

5. Conclusions

Neutral cesium deposition with simultaneous primary ion bombardment produces a significant increase of the useful yields of negative secondary ions and thus of the analysis sensitivity compared to traditional Cs^+ primary ion bombardment. The overall useful yield variations with respect to the parameters τ and T characterizing the cesium surface concentration agree qualitatively with the predictions of the electron tunneling model. At maximal cesium surface concentrations, quantitative analyses become possible for elements with high electron affinities. For other elements a significant increase of the analysis sensitivity is achieved. Furthermore, neutral cesium deposition with simultaneous ion bombardment has been applied successfully to typical SIMS applications like depth profiling. Nevertheless different fundamental aspects linked to sputtering and the Cs^0 deposition remain unexplored and will be discussed in later papers.

Acknowledgment

This work has been supported by the "Ministère de la Culture, de l'Enseignement Supérieur et de la Recherche" of Luxembourg.

References

[1] H.A. Storms, K.F. Brown, J.D. Stein, Anal. Chem. 49 (1977) 2023.
[2] G. Stingeder, Anal. Chim. Acta 297 (1994) 231.
[3] M.A. Karolewski, R.G. Cavell, Appl. Surf. Sci. 193 (2002) 11.
[4] K. Wittmaack, Surf. Sci. 126 (1983) 573.
[5] M. Scheffler, C. Stampfl, Handbook of Surface Science, 1999, p. 286.
[6] A. Hohlfeld, M. Sunjic, K. Horn, J. Vac. Sci. Technol. A 5 (4) (1987) 679.
[7] B. Kierren, D. Paget, J. Vac. Sci. Technol. A 15 (4) (1997) 2074.
[8] D. Heskett, T. Maeda, A.J. Smith, W.R. Graham, N.J. DiNardo, E.W. Plummer, J. Vac. Sci. Technol. B 7 (4) (1989) 915.
[9] P. Soukiassian, L. Spiess, K.M. Schirm, P.S. Mangat, J.A. Kubby, S.P. Tang, A.J. Freeman, J. Vac. Sci. Technol. B 11 (4) (1993) 1431.
[10] H. Gnaser, Phys. Rev. B 54 (23) (1996) 16456.
[11] T. Kan, K. Mitsukawa, T. Ueyama, M. Takada, T. Yasue, T. Koshikawa, J. Surf. Anal. 5 (1) (1999) 52.
[12] P.A.W. van der Heide, Appl. Surf. Sci. 157 (2000) 191.
[13] H. Gnaser, Phys. Rev. B 63 (2001) 45415.
[14] P.A.W. van der Heide, Nucl. Instrum. Methods Phys. Res. B 194 (2002) 489.
[15] T. Mootz, B. Rasser, P. Sudraud, E. Niehuis, T. Wirtz, W. Bieck, H.-N. Migeon, in: A. Benninghoven, P. Bertrand, H.-N. Migeon, H.W. Werner (Eds.), Secondary Ion Mass Spectrometry SIMS XII, Elsevier, Amsterdam, 2000, p. 233.
[16] T. Wirtz, B. Duez, H.-N. Migeon, H. Scherrer, Int. J. Mass Spectrom. 209 (2001) 57.
[17] P. Philipp, T. Wirtz, H.-N. Migeon, H. Scherrer, Appl. Surf. Sci. 231–232 (2004) 754.
[18] T. Wirtz, H.-N. Migeon, H. Scherrer, Int. J. Mass Spectrom. 225 (2003) 135.
[19] T. Wirtz, H.-N. Migeon, Surf. Sci. 557 (2004) 57.
[20] T. Wirtz, H.-N. Migeon, Surf. Sci. 561 (2004) 200.
[21] T. Wirtz, H.-N. Migeon, Appl. Surf. Sci. 231–232 (2004) 940.
[22] M. Bernheim, J. Rebière, G. Slodzian, SIMS II (1979) 40.
[23] M. Bernheim, G. Slodzian, SIMS VI (1987) 139.
[24] M. Bernheim, F. Le Bourse, Nucl. Instrum. Methods Phys. Res. B 27 (1987) 94.
[25] H.B. Michaelson, J. Appl. Phys. 48 (11) (1977) 4729.
[26] R.L. Gerlach, T.N. Rhodin, Surf. Sci. 19 (1970) 403.
[27] T. Wirtz, H.-N. Migeon, Appl. Surf. Sci. 231–232 (2004) 743.
[28] E. Chason, T.M. Mayer, Appl. Phys. Lett. 62 (4) (1993) 363.
[29] S.W. MacLaren, J.E. Baker, N.L. Finnegan, C.M. Loxton, J. Vac. Sci. Technol. A 10 (3) (1992) 468.
[30] J.J. Vajo, R.E. Doty, E.-H. Cirlin, J. Vac. Sci. Technol. A 14 (5) (1996) 2709.
[31] J. Erlebacher, M.J. Aziz, E. Chason, M.B. Sinclair, J.A. Floro, J. Vac. Sci. Technol. A 18 (1) (2000) 115.
[32] M.A. Makeev, A.L. Barabasi, Nucl. Instrum. Methods Phys. Res. B 222 (2004) 316;
M.A. Makeev, A.L. Barabasi, Nucl. Instrum. Methods Phys. Res. B 222 (2004) 335.
[33] H. Gnaser, Appl. Surf. Sci. 203–204 (2003) 78.
[34] P.A.W. van der Heide, M.S. Lim, S.S. Perry, J. Bennett, Appl. Surf. Sci. 203–204 (2003) 156.
[35] P.A.W. van der Heide, Surf. Sci. 447 (2000) 62.
[36] T. Matsunaga, S. Yoshikawa, K. Tsukamoto, Surf. Sci. 515 (2002) 390.